

Mass-Spectrometric Study on Ion-Molecule Reactions of CH_5^+ , C_2H_5^+ , and C_3H_5^+ with Monosubstituted Benzenes Carrying a Carbonyl Group

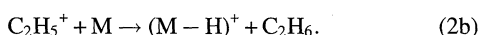
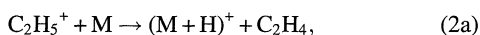
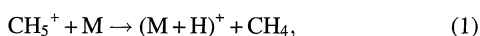
Masaharu Tsuji* and Yukio Nishimura

Institute of Advanced Material Study, Kyushu University, Kasuga, Fukuoka 816

(Received August 19, 1997)

The gas-phase ion-molecule reactions of CH_5^+ , C_2H_5^+ , and C_3H_5^+ with five monosubstituted benzenes carrying a carbonyl group (PhCOX : $\text{X}=\text{H}$, CH_3 , C_2H_5 , Ph , COPh) have been studied using an ion-trap type of GC/MS at a low CH_4 pressure. The major product channels are proton transfer to the O-atom in a substituent, with or without further decomposition due to the elimination of CO , PhH , or $(\text{PhH}+\text{CO})$. Small amounts of initial adduct ions and their decomposition products are found in some reactions with C_3H_5^+ . The reaction mechanism is discussed, based on product ion distributions and semi-empirical calculations of the energies of intermediates and products.

Chemical ionization (CI) has been widely used as a soft ionization method of a reagent in mass spectroscopy.^{1,2)} When CH_4 is used as a CI gas, the major reactant ions are CH_5^+ , C_2H_5^+ , and C_3H_5^+ .³⁾ Most CI mass spectra using CH_4 have been measured at a high CH_4 pressure of about 1 Torr (1 Torr = 133.322 Pa) without separating reactant ions. Therefore, the relative contribution of each reactant ion to the product ions could not be determined; the collisional stabilization by the CI gas often takes part in the formation of product ions. The relative concentrations of CH_5^+ , C_2H_5^+ , and C_3H_5^+ were measured to be 48, 41, and 6%, respectively, under a typical CH_4 pressure of about 1 Torr.³⁾ The relative concentrations of the former two ions are higher than the last ion, and the reactivity of the former two ions are higher than the last ion.²⁾ Therefore, the major reactant ions in the CH_4 atmosphere are CH_5^+ and C_2H_5^+ , which can induce the following proton transfer and hydride transfer in the reaction with a reagent molecule M:



We have recently studied CI mass spectra of benzene and toluene at a low CH_4 pressure by separating the reactant CH_5^+ , C_2H_5^+ , and C_3H_5^+ ions.⁴⁾ Although Munson and Field⁵⁾ have observed such initial adduct ions as $(\text{M}+\text{C}_2\text{H}_5)^+$ and $(\text{M}+\text{C}_3\text{H}_5)^+$ in CI mass spectra measured at a high CH_4 gas pressure of 1 Torr, they could not be found in our study. It was therefore concluded that the collisional stabilization by the reactant CH_4 gas participated in the formation of the adduct ions in their measurements. CI mass spectra of some benzene derivatives having a carbonyl group have been measured at a high CH_4 pressure without separating reactant ions.⁶⁾ In the present work, ion-molecule reactions of CH_5^+ , C_2H_5^+ , and C_3H_5^+ with PhCOX ($\text{X}=\text{H}$, CH_3 , C_2H_5 , Ph ,

COPh) were studied at a low CH_4 pressure using an ion-trap type of GC/MS by separating reactant ions. The reaction mechanism of monosubstituted benzenes carrying a carbonyl group for the hydrocarbon ions is discussed based on product ion distributions and semi-empirical calculations of potential energies of reaction pathways.

Experimental

CI mass spectra were obtained by using an ion-trap type of Hitachi M7200 GC/MS in a selected reactant ion mode. The time for storing a reactant ion was 5 ms and the reaction time was 20 ms. The ion-trap cell was kept at $\leq 170^\circ\text{C}$. The reagents were diluted in hexane and injected into the GC with a high-purity carrier He gas. The partial pressures of He and CH_4 in the ion-trap cell were estimated to be 5×10^{-5} and 7×10^{-5} Torr, respectively. The reactant ions, produced by electron-impact ionization of CH_4 followed by secondary ion-molecule reactions, were expected to be thermalized by collisions with the carrier He gas and CH_4 before CI of a reagent. In order to confirm this prediction, the CI mass spectra of PhCOPh were measured by changing the storing time of the reactant CH_5^+ or C_2H_5^+ ion between 5 and 15 ms. The CI mass spectra were independent of the storing time of the reactant ion, leading us to conclude that the above prediction is valid. The CI mass spectra were measured at low reagent concentrations of about $1000\text{--}5000 \text{ pg cm}^{-3}$ in order to reduce secondary ion-molecule reactions.

The heats of formation are known for the reactant ions, reagents, and some stable products obtained in this work.⁷⁾ However, there are many species whose ΔH° values are unknown. These values were calculated by using a semi-empirical MNDO method (MOPAC Ver. 6.0) in order to describe potential-energy diagram of the reaction pathways. Thermochemical data used in this work are summarized in Table 1.

Results and Discussion

The observed product ions and their branching ratios in the reactions of CH_5^+ , C_2H_5^+ , and C_3H_5^+ with PhCOX ($\text{X}=\text{H}$, CH_3 , C_2H_5 , Ph , COPh) are summarized in Table 2. The un-

Table 1. Thermochemical Data Used in This Work

Molecules		ΔH°		Ref.
		kJ mol^{-1}	eV	
CH_4		-74.5	-0.772	Ref. 7
CH_5^+		905	9.38	Ref. 7
C_2H_5^+		902	9.36	Ref. 7
C_2H_4		52.2	0.541	Ref. 7
C_2H_6		-84	-0.87	Ref. 7
CO		-110.53	-1.146	Ref. 7
CHO^+		825.6	8.561	Ref. 7
COCH_3^+		653	6.77	Ref. 7
COC_2H_5^+		591	6.13	Ref. 7
COC_2H_3^+		751	7.78	Ref. 7
PhH		82.9	0.859	Ref. 7
PhH_2^+		854	8.85	Ref. 7
PhCHO		-37	-0.38	Ref. 7
PhCOCH_3		-86.6	-0.898	Ref. 7
PhCOC_2H_5		-109	-1.13	Ref. 7
PhCOPh		50	0.52	Ref. 7
PhCOCOPh		-56	-0.58	Ref. 7
PhCO^+		705	7.31	Ref. 7
PhCOCO^+		710.08	7.359	This work
$(\text{PhCH}_3)\text{H}^+$	(ortho-protonated)	833.11	8.635	This work
$(\text{PhCH}_3)\text{H}^+$	(meta-protonated)	829.47	8.597	This work
$(\text{PhCH}_3)\text{H}^+$	(para-protonated)	837.67	8.682	This work
$(\text{PhCH}_3)\text{H}^+$	(ipso-protonated)	857.93	8.892	This work
$(\text{PhCHO})\text{H}^+$	(O-protonated)	655	6.789	Ref. 7
$(\text{PhCHO})\text{H}^+$	(ortho-protonated)	768.39	7.964	This work
$(\text{PhCHO})\text{H}^+$	(meta-protonated)	764.12	7.920	This work
$(\text{PhCHO})\text{H}^+$	(para-protonated)	768.94	7.970	This work
$(\text{PhCHO})\text{H}^+$	(ipso-protonated)	777.58	8.059	This work
$(\text{PhCOCH}_3)\text{H}^+$	(O-protonated)	584	6.053	Ref. 7
$(\text{PhCOCH}_3)\text{H}^+$	(ortho-protonated)	733.69	7.604	This work
$(\text{PhCOCH}_3)\text{H}^+$	(meta-protonated)	729.71	7.563	This work
$(\text{PhCOCH}_3)\text{H}^+$	(para-protonated)	733.27	7.600	This work
$(\text{PhCOCH}_3)\text{H}^+$	(ipso-protonated)	744.82	7.720	This work
$(\text{PhCOC}_2\text{H}_5)\text{H}^+$	(O-protonated)	607.56	6.297	This work
$(\text{PhCOC}_2\text{H}_5)\text{H}^+$	(ortho-protonated)	732.73	7.594	This work
$(\text{PhCOC}_2\text{H}_5)\text{H}^+$	(meta-protonated)	726.53	7.530	This work
$(\text{PhCOC}_2\text{H}_5)\text{H}^+$	(para-protonated)	737.46	7.643	This work
$(\text{PhCOC}_2\text{H}_5)\text{H}^+$	(ipso-protonated)	723.48	7.498	This work
$(\text{PhCOPh})\text{H}^+$	(O-protonated)	699.07	7.245	This work
$(\text{PhCOPh})\text{H}^+$	(ortho-protonated)	863.67	8.951	This work
$(\text{PhCOPh})\text{H}^+$	(meta-protonated)	859.40	8.907	This work
$(\text{PhCOPh})\text{H}^+$	(para-protonated)	861.57	8.930	This work
$(\text{PhCOPh})\text{H}^+$	(ipso-protonated)	871.62	9.034	This work
$(\text{PhCOCOPh})\text{H}^+$	(O-protonated)	652.77	6.766	This work
$(\text{PhCOCOPh})\text{H}^+$	(ortho-protonated)	754.20	7.817	This work
$(\text{PhCOCOPh})\text{H}^+$	(meta-protonated)	748.38	7.756	This work
$(\text{PhCOCOPh})\text{H}^+$	(para-protonated)	753.91	7.814	This work
$(\text{PhCOCOPh})\text{H}^+$	(ipso-protonated)	765.67	7.936	This work
$(\text{PhCOC}_2\text{H}_3)\text{H}^+$	(O-protonated)	716.48	7.426	This work
$(\text{PhCOC}_2\text{H}_3)\text{H}^+$	(ortho-protonated)	824.61	8.547	This work
$(\text{PhCOC}_2\text{H}_3)\text{H}^+$	(meta-protonated)	821.01	8.509	This work
$(\text{PhCOC}_2\text{H}_3)\text{H}^+$	(para-protonated)	824.11	8.541	This work
$(\text{PhCOC}_2\text{H}_3)\text{H}^+$	(ipso-protonated)	837.00	8.675	This work

certainties of the branching ratios are estimated to be within $\pm 7\%$.

Benzaldehyde: In the $\text{CH}_5^+/\text{PhCHO}$ reaction, the PhH_2^+ and $(\text{PhCHO})\text{H}^+$ ions are observed with branching ratios of 62 and 38%, respectively. Beside these two ions,

small amounts of the PhCO^+ and C_4H_3^+ ions are found in the $\text{C}_2\text{H}_5^+/\text{PhCHO}$ reaction. It should be noted that the $\text{PhH}_2^+/(\text{PhCHO})\text{H}^+$ ratio decreases greatly from 1.6 to 0.29, when the reactant ion is changed from CH_5^+ to C_2H_5^+ . In the $\text{C}_3\text{H}_5^+/\text{PhCHO}$ reaction, the number of product chan-

Table 2. Branching Ratios (%) of Product Ions in the Reactions of CH_5^+ , C_2H_5^+ , and C_3H_5^+ with PhCOX ($\text{X}=\text{H}$, CH_3 , C_2H_5 , Ph , COPh)

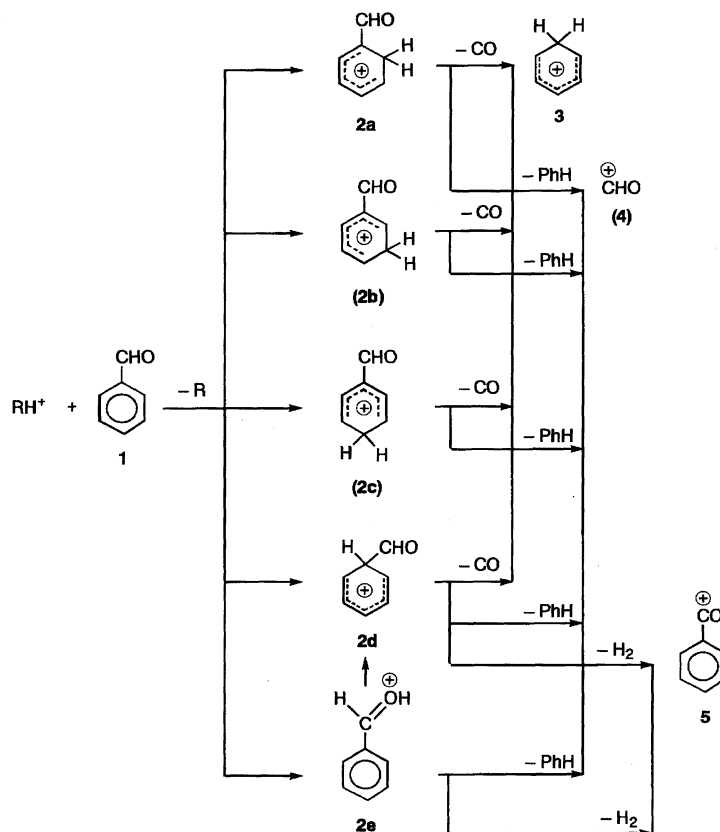
Reagents	PhCHO			PhCOCH ₃			PhCOC ₂ H ₅			PhCOPh			PhCOCOPh		
Reactant ions	CH_5^+	C_2H_5^+	C_3H_5^+	CH_5^+	C_2H_5^+	C_3H_5^+	CH_5^+	C_2H_5^+	C_3H_5^+	CH_5^+	C_2H_5^+	C_3H_5^+	CH_5^+	C_2H_5^+	C_3H_5^+
Product ions															
$(\text{M}+\text{C}_3\text{H}_5)^+$						0.4						8.7			
$(\text{M}+\text{C}_3\text{H}_5-\text{PhH})^+$												3.0			
$(\text{M}+\text{C}_3\text{H}_5-\text{PhCHO})^+$															3.4
$(\text{M}+\text{H})^+$	38	73	26	28	76	22	30	42	12	24	62	23	1.6	9.3	12
$(\text{M}-\text{H})^+$							7.2	6.4							
PhCOCO ⁺														2.5	
PhCO ⁺		2.0	21	2.9	7.2	3.8	4.2	3.9	2.4	76	38	48	98	85	63
C_7H_7^+			6.5					1.7	3.3			2.0			
PhH ₂ ⁺	62	21	15		2.8	2.7									6.3
C_4H_3^+		4.2	23		6.9	7.8		3.6	14			12		3.3	13
C_4H_2^+			9.1			2.2			3.0			2.5			2.1
COHCH ₃ ⁺						1.2									
COCH ₃ ⁺				69	7.6	60									
COC ₂ H ₅ ⁺							51	37	56						
COC ₂ H ₃ ⁺							7.2	5.1	9.0						

Uncertainties are within $\pm 7\%$.

nels increases, and the C_7H_7^+ and C_4H_2^+ ions, which are absent in the $\text{CH}_5^+/\text{PhCHO}$ and $\text{C}_2\text{H}_5^+/\text{PhCHO}$ reactions, are found. There are three possible C_3H_5^+ ions. They are $\text{CH}_2=\text{CHCH}_2^+$, $\text{CH}_3\text{C}=\text{CH}_2^+$, and protonated cyclopropene ion with $\Delta H^\circ=946, 969$, and 1069 kJ mol^{-1} , respectively.⁷⁾ The most stable $\text{CH}_2=\text{CHCH}_2^+$ isomer may be most signifi-

cant under the present experimental condition.

Possible reaction mechanisms of the $\text{CH}_5^+/\text{PhCHO}$ and $\text{C}_2\text{H}_5^+/\text{PhCHO}$ reactions are given in Scheme 1. The $(\text{PhCHO})\text{H}^+$ ion can be formed through a proton transfer to the benzene ring or the lone-pair electrons of the O-atom in the substituent. The electron-withdrawing effect of the CHO



Scheme 1. Numbers in parentheses are minor or unimportant intermediates and products.

group will suppress the formation of Wheland-type adduct ions **2a**—**2d**, while a high reactivity of the lone-pair electrons on the oxygen atom will yield O-protonated ion **2e** preferentially. Actually, we have recently studied ion-molecule reactions of a typical carbocation, CF_3^+ , with $PhCOX$ ($X=H, CH_3, C_2H_5$), and found that almost all electrophilic attack (93—96%) occurs on the O-atom in the substituent.⁸⁾ Since the protonation is a reversible process with a low energy barrier, it will be controlled thermochemically. Figures 1 and 2 show the potential energy diagrams of the protonation/molecular-elimination pathways in the $CH_5^+/PhCHO$ and $C_2H_5^+/PhCHO$ reactions. It is clear from Figs. 1 and 2 that the O-protonated ion **2e** is much more stable than ring-protonated ions **2a**—**2d**. These facts support our prediction that **2e** is a dominant $(PhCHO)H^+$ ion. The $PhH_2^+/(PhCHO)H^+$ ratio in the $C_2H_5^+/PhCHO$ reaction is lower than that in the $CH_5^+/PhCHO$ reaction. This can be explained by a higher proton affinity of C_2H_4 (7.1 eV) than that of CH_4 (5.7 eV), so that a lower excess energy is released in the former protonation reaction (Figs. 1 and 2).

It is highly likely that the PhH_2^+ ion (**3**) is formed by loss of CO from ring-protonated ions **2a**—**2d**, as shown in Scheme 1. The initial protonation is expected to occur preferentially in the substituent. It is, therefore, reasonable to assume that almost all precursor ring-protonated ions are not produced directly but they are formed via such an intramolecular proton transfer as **2e**→**2a** and **2e**→**2d**. Only the intramolecular proton transfer from **2e** to **2d** is shown in Scheme 1 and Figs. 1 and 2 for the sake of clarity. The $PhCO^+$ ion (**5**) can be formed by loss of H_2 from **2d** and/or **2e**. Although the ΔH° value of $PhCO^+$ (**5**)+ H_2 is lower than that of PhH_2^+ (**3**)+CO (Figs. 1 and 2), the branching ratio of

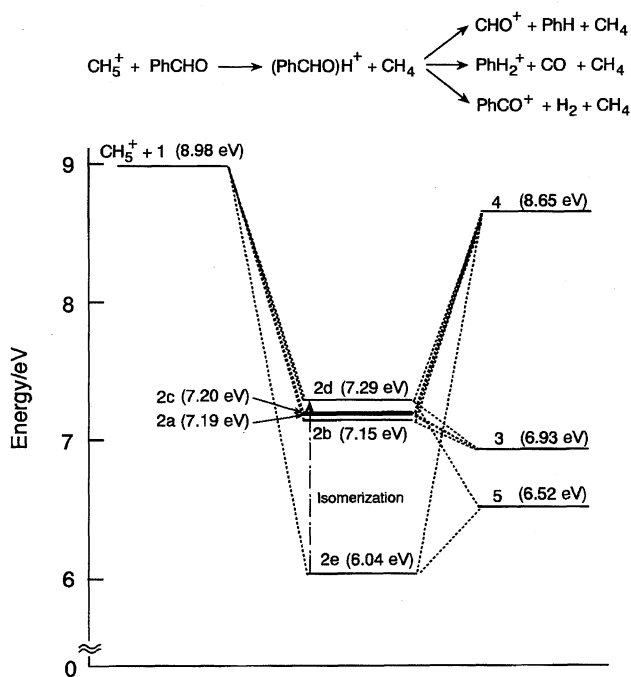


Fig. 1. A potential-energy diagram for the protonation/dissociation pathways in the $CH_5^+/PhCHO$ system.

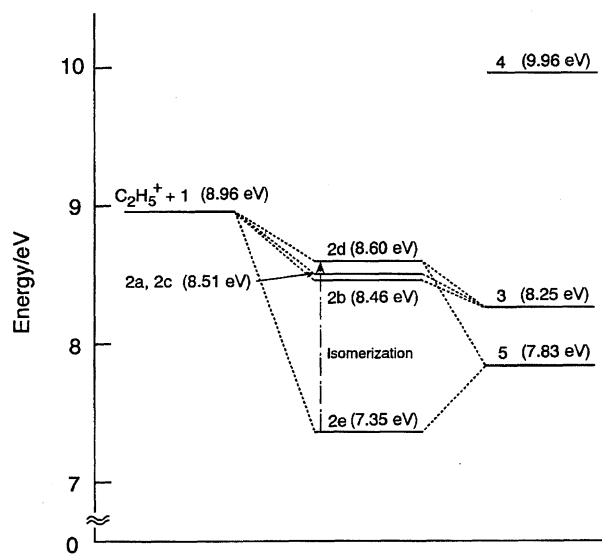
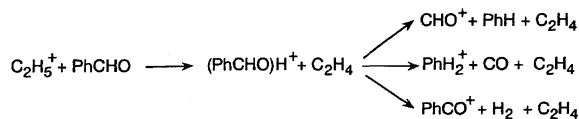


Fig. 2. A potential-energy diagram for the protonation/dissociation pathways in the $C_2H_5^+/PhCHO$ system.

5 is either zero or very small in the CH_5^+ and $C_2H_5^+$ reactions. In general, elimination channels from protonated ions are expected to be controlled kinetically, because the elimination processes are irreversible. Thus, the small branching ratios of **5** are attributed to higher energy barriers for the formation of **5** from **2d** and **2e** than those for the formation of **3** from **2a**—**2d**. Although the formation of CHO^+ (**4**) is energetically accessible in the CH_5^+ reaction, it cannot be detected. The lack of **4** in the CH_5^+ reaction is explained by the fact that the potential energy for the formation of **4** is much higher than that of **3**, so that an efficient conversion of the excess internal energy to dissociation energy is required for the formation of **4** (Fig. 1). On the other hand, the lack of **4** in the $C_2H_5^+$ reaction is due to the endothermicity of its formation (Fig. 2).

Methyl Phenyl Ketone: A possible reaction scheme and the potential-energy diagrams of the $CH_5^+/PhCOCH_3$ and $C_2H_5^+/PhCOCH_3$ reactions are given in Scheme 2 and Figs. 3 and 4, respectively. If the reaction mechanism of the $CH_5^+/PhCOCH_3$ and $C_2H_5^+/PhCOCH_3$ reactions is similar to that of the $CH_5^+/PhCHO$ and $C_2H_5^+/PhCHO$ reactions, the $(PhCOCH_3)H^+$ ion (**7**) and the $PhHCH_3^+$ ion (**8**) are expected to be produced preferentially. Although the former ion was found as a major product ion, the latter ion could not be detected. Since **7e** is thermochemically most favorable among possible $(PhCOCH_3)H^+$ ions (**7a**—**7e**) due to electron-withdrawing properties of the CH_3CO group, it will be a major $(PhCOCH_3)H^+$ ion. On the basis of energy-level diagrams shown in Figs. 3 and 4, the formation of **8a**—**8d** is energetically allowed and the potential energies of **8a**—**8d**+CO are comparable with those of the precursor **7a**—**7d** ions. We have recently found that the $PhHCH_3^+$ ion is produced in the

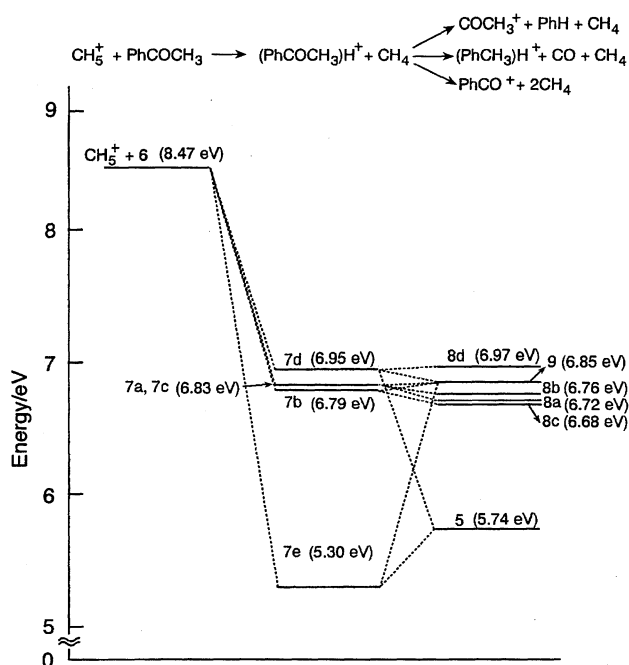
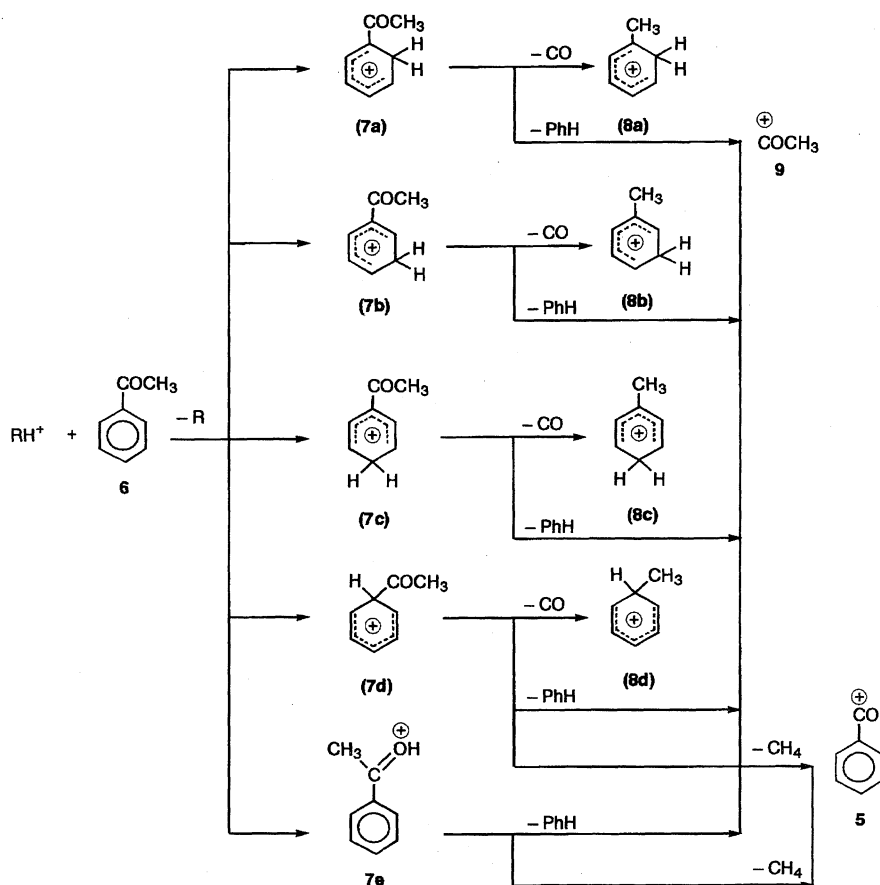


Fig. 3. A potential-energy diagram for the protonation/dissociation pathways in the $\text{CH}_5^+ + \text{PhCOCH}_3$ system.

reactions of CH_5^+ and C_2H_5^+ with PhCH_3 with high branching ratios of 93 and 89%, respectively.⁴⁾ This implies that the PhHCH_3^+ ion is a stable detectable ion. Thus, the lack

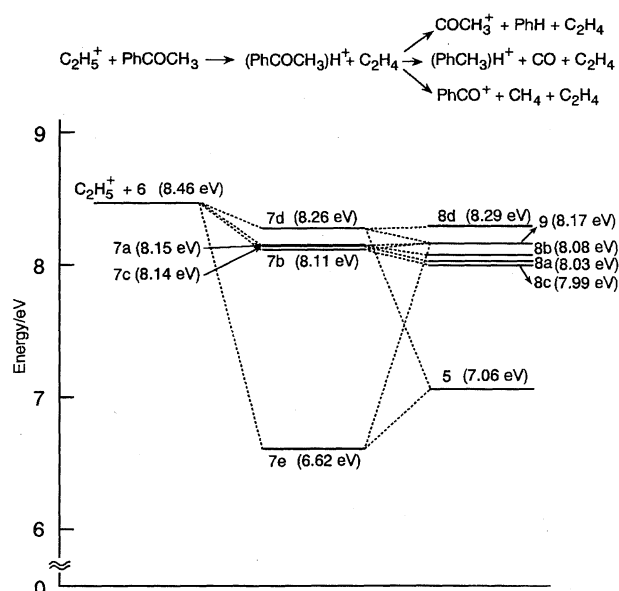


Fig. 4. A potential-energy diagram for the protonation/dissociation pathways in the $\text{C}_2\text{H}_5^+ + \text{PhCOCH}_3$ system.

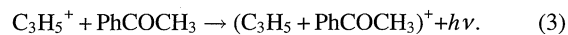
of **8a–8d** from PhCOCH_3 suggests that the CO elimination from **7a–7d** due to the migration of a heavy CH_3 group to the benzene ring is less efficient.

It should be noted that the COCH_3^+ ion (**9**) is found as

a dominant product ion (69%) in the CH_5^+ reaction. It can be produced through the elimination of PhH from the ring protonated ions (7a—7d) and the O-protonated ion (7e). Since the initial protonation occurs preferentially to the O-atom, it is highly likely that 9 is dominantly produced through 7e. The branching ratio of $COCH_3^+$ is very small in the $C_2H_5^+$ reaction in comparison with that in the CH_5^+ reaction. This is attributed to a lower excess energy in the $C_2H_5^+$ reaction, so that an efficient conversion of the excess internal energy to the dissociation energy is required for the formation of $COCH_3^+$ (Fig. 4). Small amounts of the $PhCO^+$ ion (5) are found in the CH_5^+ and $C_2H_5^+$ reactions. Although 5 can be formed by loss of CH_4 from the ipso-protonated ion 7d and the ring-protonated ion 7e, the major precursor ion is expected to be the more stable latter ion.

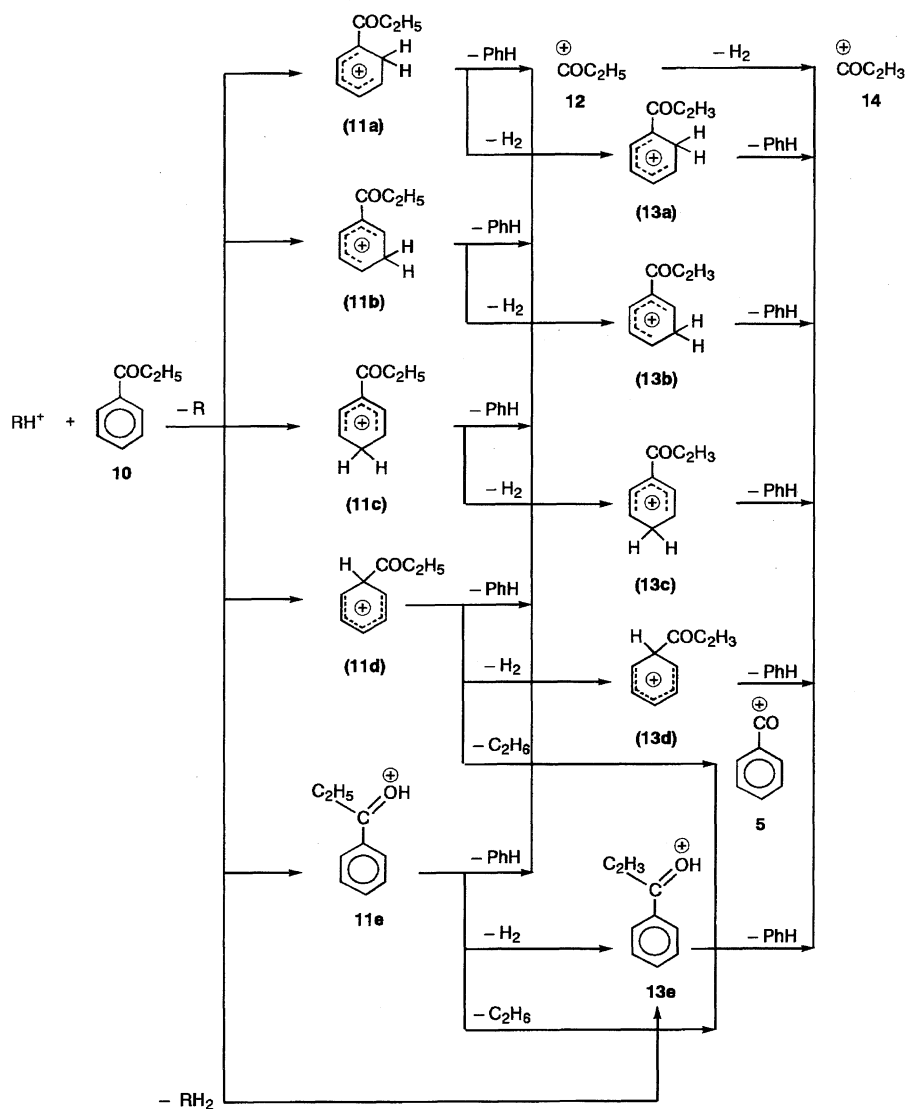
The number of product channels increases in the $C_3H_5^+/PhCOCH_3$ reaction, as found in the $C_3H_5^+/PhCHO$ reaction. It should be noted that a small amount of the initial adduct $(M+C_3H_5)^+$ ion is found. Since the collisional stabilization is insignificant in the present experimental con-

ditions, it may be stabilized by radiative association, as reported for the reactions of NO^+ with carbonyl compounds:⁹⁾

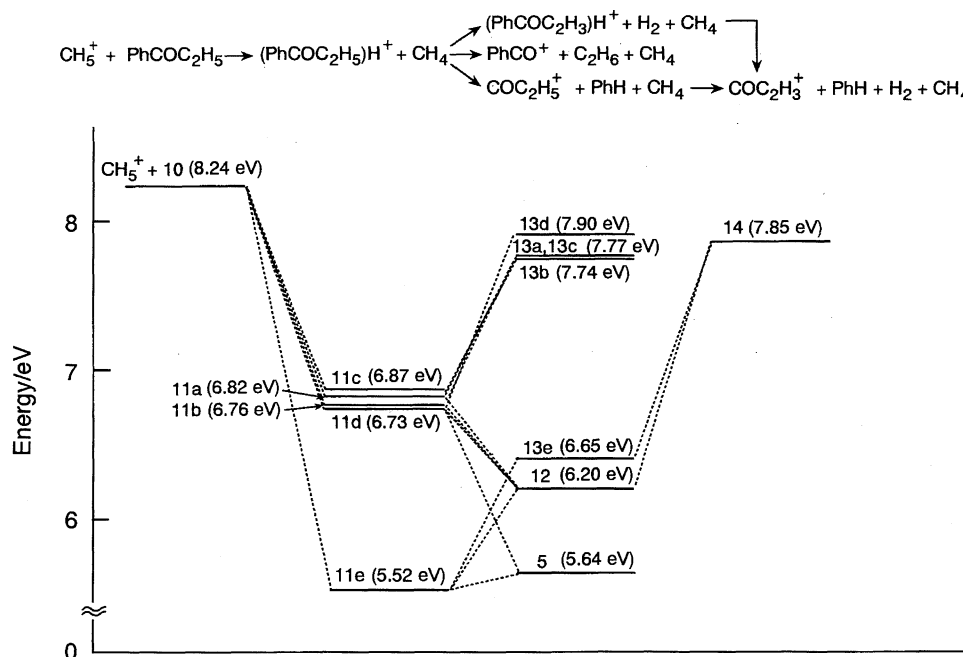
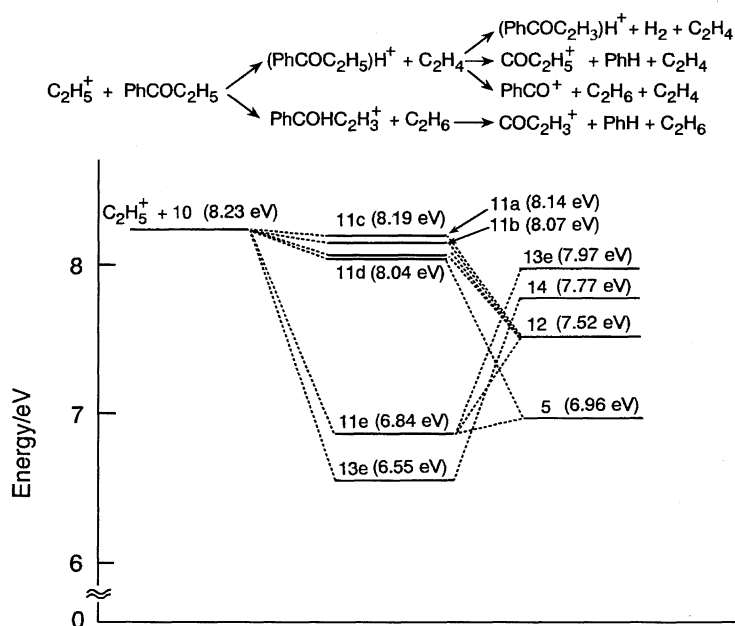


Ethyl Phenyl Ketone: Major products in the $CH_5^+/PhCOC_2H_5$ and $C_2H_5^+/PhCOC_2H_5$ reactions are the $(PhCOC_2H_5)H^+$ and $COC_2H_5^+$ ions, indicating that the reaction mechanism is similar to that of $PhCOCH_3$. In Scheme 3 and Figs. 5 and 6 are shown a possible reaction scheme and the potential-energy diagrams of the $CH_5^+/PhCOC_2H_5$ and $C_2H_5^+/PhCOC_2H_5$ reactions. The $COC_2H_5^+$ group has electron-withdrawing properties. Therefore, the major $(PhCOC_2H_5)H^+$ ion will be more stable O-protonated ion (11e), and the $COC_2H_5^+$ ion (12) is dominantly produced via loss of PhH from 11e. The $COC_2H_5^+/(PhCOC_2H_5)H^+$ ratio in the $C_2H_5^+/PhCOC_2H_5$ reaction is lower than that in the $CH_5^+/PhCOC_2H_5$ reaction by a factor of 1.9 due to a lower excess energy (Figs. 5 and 6).

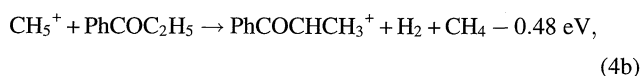
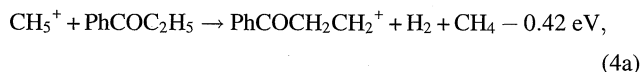
Small amounts of the $(M-H)^+ = PhCOC_2H_4^+$, $PhCO^+$, and $COC_2H_3^+$ ions are found in the CH_5^+ and $C_2H_5^+$ re-



Scheme 3.

Fig. 5. A potential-energy diagram for the protonation/dissociation pathways in the $\text{CH}_5^+ + \text{PhCOC}_2\text{H}_5$ system.Fig. 6. A potential-energy diagram for the protonation/dissociation pathways in the $\text{C}_2\text{H}_5^+ + \text{PhCOC}_2\text{H}_5$ system.

actions. Possible candidates of the $(\text{M}-\text{H})^+$ ions are ring-protonated ions **13a**–**13d** and the O-protonated ion **13e** in the CH_5^+ reaction, because the formation of $\text{PhCOCH}_2\text{CH}_2^+$ and PhCOCHCH_3^+ are endoergic:



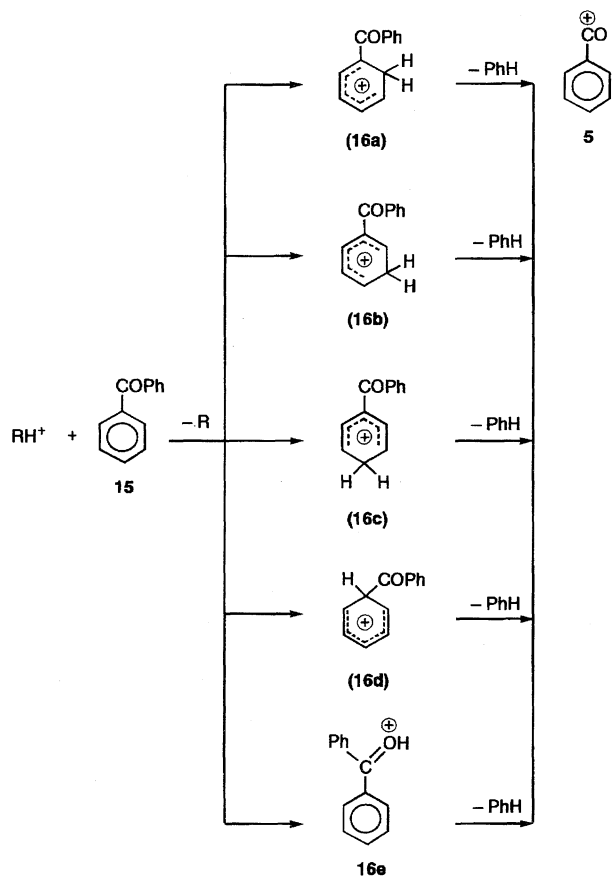
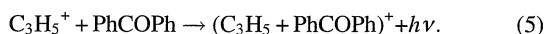
Among them, the ion **13e**, formed by the H_2 elimination from **11e**, will be a dominant $(\text{M}-\text{H})^+$ ion in the CH_5^+ reaction.

Only the formation of **13e** is energetically possible in the C_2H_5^+ reaction (Fig. 6). There are two possible processes for the formation of **13e** in the C_2H_5^+ reaction, as shown in Scheme 3. One is protonation to the O-atom followed by loss of H_2 , as found in the CH_5^+ reaction, and the other is hydride abstraction from the C_2H_5 group involving intramolecular proton transfer from the C_2H_4 group to the O-atom. The formation of the COC_2H_3^+ ion (**14**) probably proceeds through loss of PhH and H_2 from the O-protonated ion (**11e**) in the CH_5^+ reaction (Scheme 3 and Fig. 5). On the other hand, such an elimination process is energetically closed for the formation of **14** in the C_2H_5^+ reaction, and only the hydride-

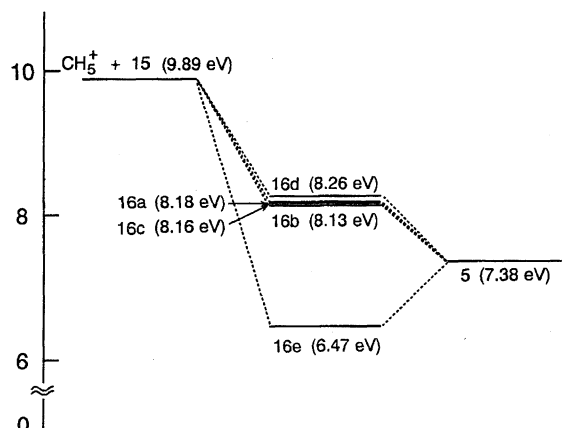
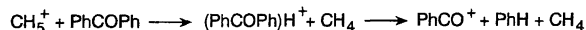
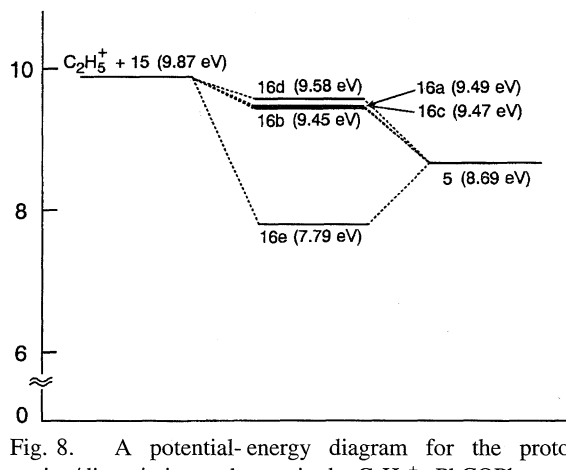
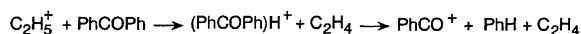
abstraction process followed by the PhH elimination is energetically possible (Scheme 3 and Fig. 6). Since the hydride-abstraction process is found to be involved in the formation of **14** in the $C_2H_5^+$ reaction, some part of **13e** will be also produced through the hydride-abstraction process. Although the $PhCO^+$ ion (**5**) can be formed through loss of C_2H_6 from the ipso-protonated ion **11d** and the O-protonated ion **11e**, the latter thermochemically favored ion will be a major precursor ion. The product ions, observed in the $C_3H_5^+$ reaction, are similar to those in the $C_2H_5^+$ reaction except for the lack of the $(M-H)^+$ and $C_4H_2^+$ ions.

Diphenyl Ketone: A possible reaction scheme and the potential-energy diagrams in the $CH_5^+/PhCOPh$ and $C_2H_5^+/PhCOPh$ reactions are given in Scheme 4 and Figs. 7 and 8, respectively. Major product ions are the $(PhCOPh)H^+$ and $PhCO^+$ ions. The dominant $(PhCOPh)H^+$ ion will be the more stable O-protonated ion (**16e**), and the $PhCO^+$ ion (**5**) is expected to be preferentially formed by the PhH elimination from **16e**. The $PhCO^+/(PhCOPh)H^+$ ratio in the $C_2H_5^+$ reaction is smaller than that in the CH_5^+ reaction by a factor of 5.2 because of a lower excess energy.

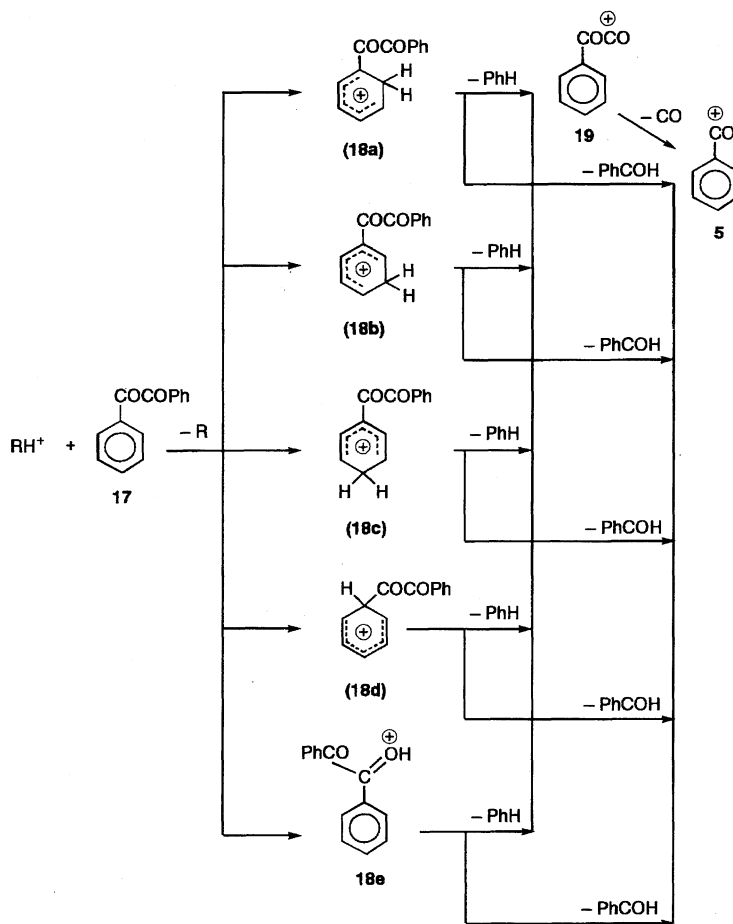
In the $C_3H_5^+/PhCOPh$ reaction, the adduct $(M+C_3H_5)^+$ ion and its decomposition product $(M+C_3H_5-PhH)^+$ ion are found. A radiative association process probably takes part in the formation of these adduct ions:



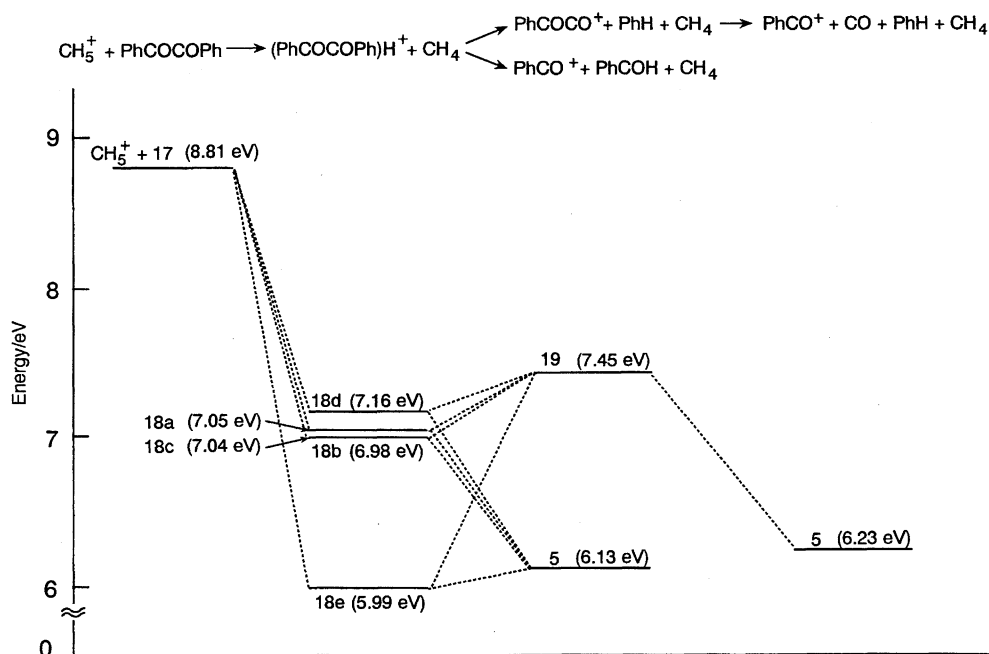
Scheme 4.

Fig. 7. A potential-energy diagram for the protonation/dissociation pathways in the $CH_5^+ + PhCOPh$ system.Fig. 8. A potential-energy diagram for the protonation/dissociation pathways in the $C_2H_5^+ + PhCOPh$ system.

Benzil: The $PhCO^+$ ion is a dominant product ion in the reactions of CH_5^+ , $C_2H_5^+$, and $C_3H_5^+$ with $PhCOCOPh$, which occupies more than 63% in all three reactions (Table 2). A small amount of the $PhCOCO^+$ ion is found only in the $C_2H_5^+$ reaction. An outstanding feature for the reactions with $PhCOCOPh$ is that the branching ratios of the $(PhCOCOPh)H^+$ ion are small in all three reactions ($\leq 12\%$). A possible reaction scheme and the potential-energy diagrams of the $CH_5^+/PhCOCOPh$ and $C_2H_5^+/PhCOCOPh$ reactions are shown in Scheme 5 and Figs. 9 and 10, respectively. The $PhCO^+$ ion (**5**) can be formed via loss of $PhCHO$ or $(PhH+CO)$ from ring-protonated ions (**18a**–**18d**) and the O-protonated ion (**18e**). It is expected to be formed though the decomposition of thermochemically more favorable ion **18e**. Although the $PhCOCO^+$ ion (**19**) is formed in the $C_2H_5^+$ reaction, it is absent in the CH_5^+ reaction. This implies that **19**, formed in the CH_5^+ reaction, completely dissociates into $PhCO^+ + CO$. It is clear from Figs. 9 and 10 that the formation of $PhCO^+ + CO$ is thermochemically much more favorable than that of $PhCOCO^+$, because the



Scheme 5.

Fig. 9. A potential-energy diagram for the protonation/dissociation pathways in the $CH_5^+ + PhCOCOPh$ system.

ΔH° value of $PhCO^+ + CO$ is lower than that of $PhCOCO^+$ by 1.22 eV. There will be a low energy barrier for the formation of $PhCO^+$ from a unimolecular decomposition of

the $(PhCO-CO)^+$ ion. Thus, an efficient decomposition of $PhCOCO^+$ into $PhCO^+ + CO$ will be the main reason for the lack of $PhCOCO^+$ in the CH_5^+ reaction and for its small

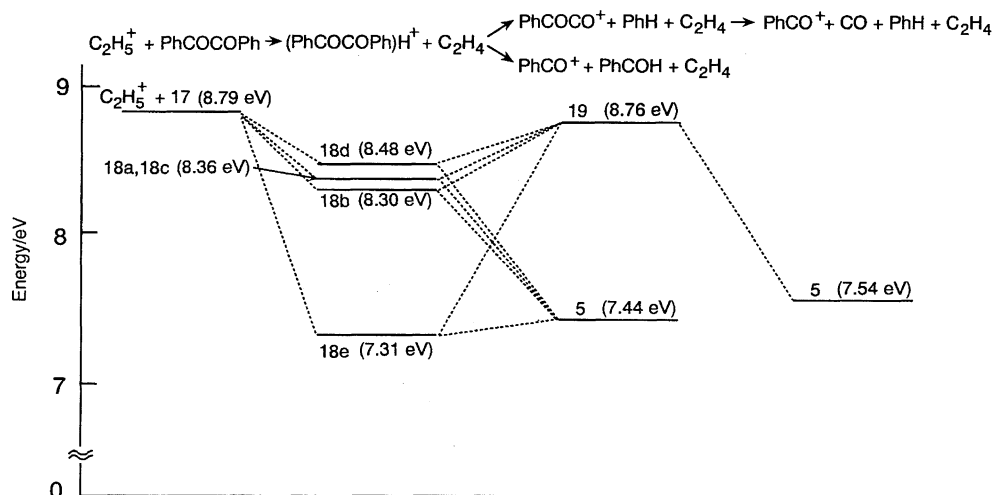


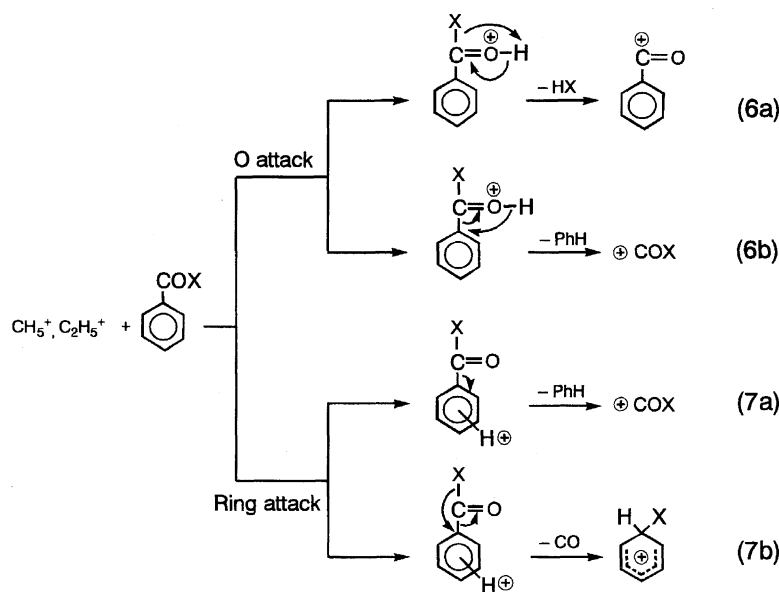
Fig. 10. A potential-energy diagram for the protonation/dissociation pathways in the $C_2H_5^+ + PhCOCOPh$ system.

branching ratio in the $C_2H_5^+$ reaction.

In the $C_3H_5^+ / PhCOCOPh$ reaction, the formation of a small amount of the adduct $(M + C_3H_5 - PhCHO)^+$ ion is observed, though the initial adduct $(M + C_3H_5)^+$ ion could not be found. In addition, the PhH_2^+ , $C_4H_3^+$, and $C_4H_2^+$ ions are also observed.

Concluding Remarks: Ion-molecule reactions of CH_5^+ , $C_2H_5^+$, and $C_3H_5^+$ with $PhCOX$ ($X=H, CH_3, C_2H_5, Ph, COPh$) have been studied using a GC/MS at a low CH_4 pressure. The product ion distributions depended strongly on the reactant ion. In general, the number of product channels increases with increasing the number of atoms in the reactant hydrocarbon ion. In some reactions with $C_3H_5^+$, initial adduct ions and decomposition products are found. Possible reaction mechanisms for CH_5^+ and $C_2H_5^+$ are summarized in Scheme 6. The major product channels are protonation with or without further decomposition due to molecular elimination. The branching ratios of $(M+H)^+$ in the $C_2H_5^+$ reaction

were larger than those in the CH_5^+ reaction, because the excess energy released in the former reaction is lower than that in the latter reaction by 1.33 eV. The protonation can occur both on the O-atom and the benzene ring. The elimination of HX and PhH from an O-protonated ion gives the $PhCO^+$ and COX^+ ions through processes (6a) and (6b), respectively. On the other hand, the elimination of PhH and CO from a ring-protonated ion gives the COX^+ and $PhHX^+$ ions through processes (7a) and (7b), respectively. Since the formation of a more stable O-protonated ion due to electron-withdrawing properties of carbonyl group is more favorable than that of ring-protonated ions, the major protonations leading to $(M+H)^+$, with and without further decomposition due to the elimination of HX and PhH , are expected to occur dominantly through processes (6a) and (6b), respectively. Actually, major product ions observed from $PhCOX$ ($X=CH_3, C_2H_5, Ph, COPh$) are $(M+H)^+$, $PhCO^+$, and COX^+ formed through processes (6a) and (6b). One reason for the



Scheme 6.

high branching ratio of PhCO^+ in the reactions with PhCOPh is that processes (6a) and (6b) give the same PhCO^+ ion. In the reactions of CH_5^+ and C_2H_5^+ with PhCOX ($\text{X}=\text{CH}_3$, C_2H_5), the branching ratio of (6b) is much larger than that of (6a). Therefore, PhCO^+ produced from PhCOPh may also be formed via process (6b). Moreover, PhCO^+ produced from PhCOCOPh is formed via the decomposition of PhCOCO^+ in process (6b). Consequently, it is highly likely that the PhH -elimination pathway (6b) takes precedence over the HX -elimination one (6a) for PhCOX ($\text{X}=\text{CH}_3$, C_2H_5 , Ph , COPh) due to a low energy barrier. It should be noted that a major product ion for PhCHO is PhH_2^+ formed through process (7b). Since the formation of its precursor ipso-protonated ion is unfavorable, PhH_2^+ is probably formed via intramolecular proton transfer from O-protonated ion to ring-protonated ions. Such intramolecular proton transfer from the substituent to ring may also occur for PhCOX ($\text{X}=\text{CH}_3$, C_2H_5 , Ph , COPh). However, the corresponding PhHX^+ ions could not be found. This is probably due to the fact that ring protonated ions decompose into $\text{COX}^+ + \text{PhH}$ because the elimination of CO is unfavorable for PhCOX with large X substituents ($\text{X}=\text{CH}_3$, C_2H_5 , Ph , COPh).

It is clear from Table 2 that the branching ratios of $(\text{M}+\text{H})^+$ in the C_3H_5^+ reaction are lower than those in the C_2H_5^+ reaction, except for the case of PhCOCOPh . Since the proton affinity of C_3H_4 (7.65 eV for $\text{CH}_2=\text{CHCH}_2$)⁷⁾ is larger than that of C_2H_4 (7.1 eV), this result cannot be explained by the excess energies released in the proton-transfer processes. One possible explanation is that most of the fragment ions are not produced by the decomposition of proton-transfer

products, but they are formed by the decomposition of the $(\text{M}+\text{C}_3\text{H}_5)^+$ adducts. In order to confirm the validity of this explanation, further experimental and theoretical studies are required.

The authors acknowledge financial support from the Mitsubishi Foundation (1996) and a Grant-in-Aid for Scientific Research No. 09440201 from the Ministry of Education, Science, Sports and Culture.

References

- 1) F. H. Field, *Acc. Chem. Res.*, **1**, 42 (1968).
- 2) J. R. Chapman, "Practical Organic Mass Spectrometry," 2nd ed, "A Guide for Chemical and Biochemical Analysis," Wiley, New York (1993).
- 3) F. H. Field and M. S. B. Munson, *J. Am. Chem. Soc.*, **87**, 3289 (1965).
- 4) M. Tsuji, E. Oda, and Y. Nishimura, *Chem. Lett.*, **1997**, 781.
- 5) M. S. B. Munson and F. H. Field, *J. Am. Chem. Soc.*, **89**, 1047 (1968).
- 6) I. Jardine and C. Fenselau, *Org. Mass Spectrom.*, **10**, 748 (1975).
- 7) S. G. Lias, J. E. Bartmess, J. F. Liebman, J. L. Holmes, R. D. Levin, and W. G. Mallard, *J. Phys. Chem. Ref. Data*, **17**, Suppl. 1 (1988).
- 8) M. Tsuji, M. Aizawa, and Y. Nishimura, *Bull. Chem. Soc. Jpn.*, **69**, 1055 (1996).
- 9) G. Weddle and R. C. Dunbar, *Int. J. Mass Spectrom. Ion Process.*, **134**, 73 (1994).